



RESEARCH ARTICLE

Oxidation Driven Reversal of PIP₂-dependent Gating in GIRK2 Channels

Sun-Joo Lee ^{1,*}, Shoji Maeda², Jian Gao¹, Colin G. Nichols ¹

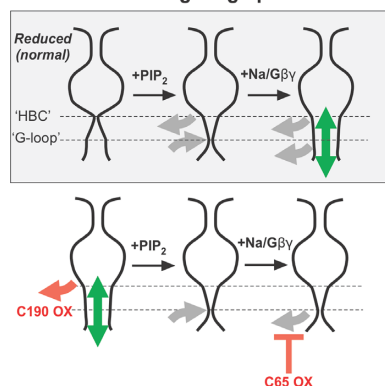
¹Department of Cell Biology and Physiology and the Center for Investigation of Membrane Excitability Diseases, Washington University School of Medicine, St. Louis, Missouri, USA and ²Department of Pharmacology, Medical School, University of Michigan, Ann Arbor, Michigan, USA

*Address correspondence to S-J.L. (e-mail: sunjoo.lee@wustl.edu)

Abstract

Physiological activity of G protein gated inward rectifier K⁺ (GIRK, Kir3) channel, dynamically regulated by three key ligands, phosphoinositol-4,5-bisphosphate (PIP₂), Gβγ, and Na⁺, underlies cellular electrical response to multiple hormones and neurotransmitters in myocytes and neurons. In a reducing environment, matching that inside cells, purified GIRK2 (Kir3.2) channels demonstrate low basal activity, and expected sensitivity to the above ligands. However, under oxidizing conditions, anomalous behavior emerges, including rapid loss of PIP₂ and Na⁺-dependent activation and a high basal activity in the absence of any agonists, that is now paradoxically inhibited by PIP₂. Mutagenesis identifies two cysteine residues (C65 and C190) as being responsible for the loss of PIP₂ and Na⁺-dependent activity and the elevated basal activity, respectively. The results explain anomalous findings from earlier studies and illustrate the potential pathophysiologic consequences of oxidation on GIRK channel function, as well as providing insight to reversed ligand-dependence of Kir and KirBac channels.

Reversal of PIP₂ gating upon oxidation



Key words: GIRK2; kir3; PIP₂; oxidation; oxidative stress; reversed gating

Submitted: 6 February 2023; Revised: 24 March 2023; Accepted: 3 April 2023

© The Author(s) 2023. Published by Oxford University Press on behalf of American Physiological Society. This is an Open Access article distributed under the terms of the Creative Commons Attribution-NonCommercial License (<https://creativecommons.org/licenses/by-nc/4.0/>), which permits non-commercial re-use, distribution, and reproduction in any medium, provided the original work is properly cited. For commercial re-use, please contact e-mail: journals.permissions@oup.com

Introduction

G protein gated inward rectifier K⁺ (GIRK, Kir3.x) channels are members of the inward rectifier K channel family, formed by hetero- or homomeric tetramers of Kir3.1–3.4 subunits. They exhibit relatively strong inward rectification, allowing K⁺ conductance at negative membrane potentials while K⁺ efflux through the channels is blocked by intracellular Mg²⁺ and polyamines¹ when cells are depolarized. GIRK channels are physiologically activated by the direct binding of Gβγ heterodimers released from heterotrimeric G-protein complexes when interacting G-protein coupled receptors [GPCRs, including GABA_B,² D2 dopamine (DA),³ and cardiac M2 muscarinic receptors⁴] are activated by their respective agonists. PI(4,5)P₂ (PIP₂), a universal activator of all Kir channels, is required to facilitate Gβγ activation.^{5,6} Ethanol⁷ and Na⁺⁸ augment PIP₂ sensitivity of the channels in a Gβγ-independent manner⁹ or with positive allostery.^{8,10}

GIRK2 (Kir3.2) prominently expresses in neurons that secrete DA, an essential regulator of voluntary movement. Neurodegenerative death of dopaminergic neurons underlies Parkinson's diseases (PD), a degenerative disorder leading to loss of motor control.¹¹ Dopaminergic neurons are subjected to oxidative stresses that are exacerbated with aging, and reducing oxidative stress via expression of scavenging proteins attenuates neurodegeneration, pointing to oxidative stress as a major underlying cause of PD.¹² Interestingly, prolonged application of L-DOPA, the most effective DA pro-drug for treating PD,¹³ leads to loss of the beneficial effect, and emergence of adverse effects. Among these is a decrease of GIRK2 activity due to oxidation of the channels by the quinone derivative of L-DOPA.¹⁴ Previous biochemical assays indicate that GIRK2 activity is sensitive to redox conditions. Consistent with this, reduction of an N-terminal cysteine (C65 of GIRK2) increases recombinant channel activity.^{15,16} In contrast, oxidation by superoxide anions has been shown to increase GIRK1 channel activity in *Xenopus laevis* oocyte in a Gβγ-independent manner.¹⁷ These contradictory results, all obtained in cellular membranes, leave it unclear exactly how oxidation/reduction affects GIRK channel activation.

In this study, we have established an in vitro assay system to tightly control both the redox state of purified GIRK2 proteins and the levels of different modulators. This allows us to show that oxidized GIRK2 acquires strikingly anomalous activities: (1) GIRK2 proteins lose PIP₂ activation; (2) the channels become highly active in the absence of any agonists, following extended exposure to oxidizing conditions; and (3) this elevated basal activity is now inhibited by PIP₂. By mutagenesis, we further show that the altered activities result from redox reactions at distinct cytoplasmic cysteine residues. The results not only provide insights to the molecular mechanisms of GIRK channel gating, and Kir channel gating more generally, but also have translational relevance for understanding disease mechanisms.

Methods

GIRK2 Expression and Purification

Experiments were carried out on a mouse GIRK2 construct (kindly provided by Dr. R. MacKinnon, The Rockefeller University, New York, NY, USA) that is truncated at both N- and C-termini and composed of residues 52 to 380. The same truncated GIRK2 construct, used for structure determinations,^{18–20} has been confirmed to generate very similar channel activities

to the full length proteins in voltage-clamped oocytes¹⁸ as well as in recombinant protein assays.^{10,20} The original construct was subcloned so that the protein is tagged C-terminally by GFP and a Flag peptide and a decahistidine (HIS10). In this report, this protein is referred to as wild type GIRK2. All point mutations were introduced to this construct via PCR with the high-fidelity DNA polymerase (Agilent, Santa Clara, CA) and confirmed by sequencing.

Wild type and mutant GIRK2 proteins were expressed in *Pichia pastoris*. Frozen yeast cells (10 GM) were broken by milling, and proteins were extracted in the lysis buffer (50 mM Tris pH 7.5, 150 mM KCl, 40 mM n-Decyl-β-D-Maltoside (DM), 2 mM β-mercaptoethanol (2-ME), DNaseI, 0.1 mg/mL AEBSF, 0.1 μg/mL Pepstatin A, 1 μg/mL Leupeptin, 1 μg/mL Apoptotinin, 1 mM PMSF). The solubilization was performed at room temperature (RT), and the rest of the purification steps were carried out at 4°C. The supernatant from a 30 000 × g centrifugation for 30 min was incubated with 250 μL cobalt resin for 2 to 3 h, then washed with 10 cv of 20 mM Imidazole buffer (50 mM Tris pH 7.5, 150 mM KCl, 4 mM DM, and 2 mM 2-ME) and with 5 cv of 40 mM Imidazole buffer (50 mM Tris pH 7.5, 150 mM KCl, 4 mM DM, 2 mM 2-ME). The elution was made by cutting off the GFP-Flag-His tag by in-house HRV-3C protease on column overnight. The eluate was concentrated and further purified by size exclusion chromatography (SEC) through Superose 6 or Superdex 200 column equilibrated with 20 mM Hepes pH 7.5, 150 mM KCl, 4 mM DM with 2 mM tris (2-chloroethyl) phosphate (TCEP), and the fractions of the tetramer peak were combined and concentrated to approximately 1 to 3 mg/mL concentrations. To prepare samples in the absence of reducing reagents, this concentrated protein was run through a second SEC equilibrated with the same buffer but in the absence of 2 mM TCEP. The fractions of the tetramer peak were combined, rapidly concentrated, and assayed without delay (Figure 1A). To prepare K⁺-free GIRK2 proteins for the experiments shown in Supplementary Fig. S2, the concentrated sample from the first SEC column was run through a second SEC column equilibrated with the SEC buffer, with 150 mM NaCl replacing 150 mM KCl. The same purification procedures were used for mutant GIRK, Kir2.2 wild type as well as A179C mutant proteins (Supplementary Fig. S5).

Gβ_{1γ2} (Gβγ) Expression and Purification

The Gβγ heterodimer was expressed in Hi5 cells using a baculovirus expression system containing the genes for Gβ1 and Gγ2 subunits.²¹ A hexa-histidine tag followed by an HRV-3C protease recognition sequence was attached to the amino-terminus of the Gβ1 subunit. Hi5 cells were infected at a density of 3.0 to 3.5 × 10⁶ cells/ml and incubated at 27°C for 48 h. After centrifugation, cells were resuspended in a lysis buffer (10 mM Tris, pH 7.5, 5 mM 2-ME, 1 mM benzamidine, and 2.5 μg/mL Leupeptin). The membrane fraction was collected by centrifugation and solubilized by Dounce homogenizer with solubilization buffer (20 mM HEPES pH 7.5, 100 mM NaCl, 1.0% sodium cholate, 0.05% dodecylmaltoside (DDM), 5 mM 2-ME, 1 mM benzamidine, and 2.5 μg/mL Leupeptin). The solubilized membrane was stirred at 4°C for 40 min, and then centrifuged to remove the insoluble fraction. The supernatant was collected and mixed with Ni-NTA resin and stirred for 2 h at 4°C. The resin was first washed in batch mode with a wash buffer (20 mM HEPES pH 7.5, 500 mM NaCl, 0.5% sodium cholate, 0.05% dodecylmaltoside, 5 mM 2-ME) to remove crude particles. Following the

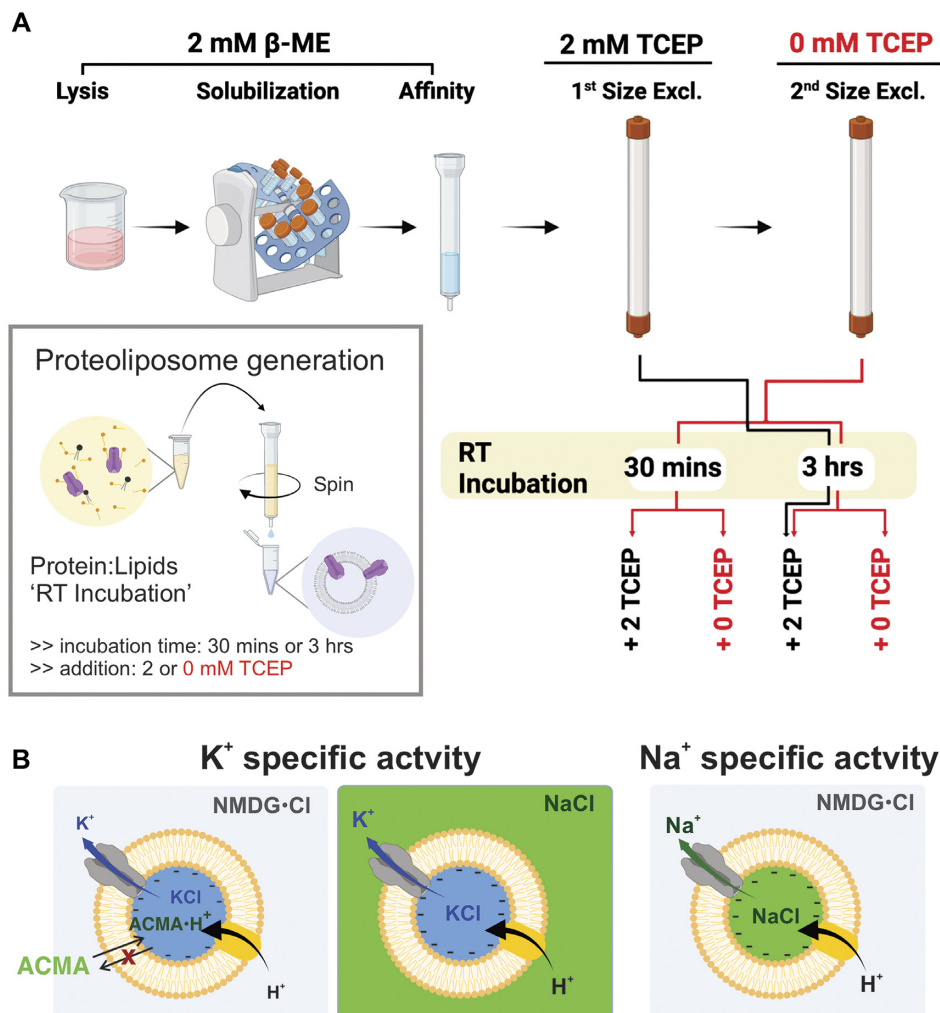


Figure 1. Strategy to test redox effect on GIRK2 activity in vitro. (A) Protein purification and in vitro flux assay scheme to tightly control the oxidation state of the purified proteins with details in “Method” section. Proteins purified without 2 mM TCEP in the oxidizing condition were subjected to experiments to test different redox conditions while protein purified with 2 mM TCEP in the reducing condition was kept in a strictly reducing condition with additional 2 mM TCEP during 3-hour RT incubation. Inset diagram describing the steps for proteoliposome formation. (B) ACMA flux assay strategies to test K^+ specific activity in the absence or presence of Na^+ by replacing external salt from NMDGCl to NaCl or to test Na^+ specific activity by replacing internal salt from KCl to NaCl while keeping the external salt with NMDGCl. Lipids forming the proteoliposomes shown in yellow, reconstituted proteins in gray blobs, proton ionophore CCCP in yellow blob. Curved arrows indicate ion or proton movements down the electrochemical gradients, and black straight arrows show the movement of ACMA across the liposome membrane with the red X mark indicating the inability of ACMA to cross the membrane when protonated and positively charged. Darker green color of ACMA-H⁺ inside the liposome indicates the quenching of the fluorophores upon protonation.

batch mode wash, the resin was further washed in an open glass column with progressively reduced sodium cholate. The protein was eluted with Ni-NTA elution buffer (20 mM HEPES pH 7.5, 100 mM NaCl, 0.05% DDM, 0.1 mM TCEP, 250 mM imidazole). To cleave off the amino terminal hexa-histidine tag, HRV-3C protease was added and the sample was dialyzed overnight against 20 mM HEPES pH 7.5, 100 mM NaCl, 0.05% dodecylmalto-side, 0.1 mM TCEP. Next day, the cleaved histidine tag, uncleaved fractions, and HRV-3C protease were removed by passing the sample through Ni-NTA resin. The flow-through fraction was concentrated and further purified by size-exclusion chromatography in a SEC buffer (20 mM HEPES pH 7.5, 100 mM NaCl, 0.05% DDM, 0.1 mM TCEP). After concentrating the peak fraction, corresponding to $G\beta\gamma$ heterodimer, 10% glycerol was added and protein aliquots were flash frozen in liquid nitrogen and kept at -80°C until use. The elution profile from the SEC column and 1D SDS gel image show highly pure dimers of $G\beta$ and $G\gamma$ (Supplementary Fig. S1D).

Flux Assay

1-palmitoyl-2-oleoyl-sn-glycero-3-phosphoethanolamine (POPE) and 1-palmitoyl-2-oleoyl-sn-glycero-3-phospho-(1'-rac-glycerol) (POPG) stocks were prepared at 10 mg/mL concentration in 20 mM HEPES, pH 7.5, 150 mM KCl, 20 mM CHAPS, 0.5 mM EGTA. They were mixed with lipids at 20% (w/w) POPG and 80% POPE with or without 1% (w/w) porcine brain L- α -phosphatidylinositol-4,5-bisphosphate (PIP₂) in 100 μL volume, and the mix was incubated at room temperature (RT) for 2 h. For experiments shown in Figure 4, 3% (w/w) brain PI(4,5)P₂ or 1 or 3% brain PI(4)P was added. For experiments shown in Supplementary Fig. S3 and S4, POPG and bPIP₂ levels were varied as shown in the figures. Then 3 μg of protein (except in experiments testing protein levels on the basal activities, Figure 2D to F and Supplementary Fig. S2 and S4) was added to each 100 μL lipid-detergent mix, giving $\sim 1:300 = P$: L mass ratio as depicted in the inset of Figure 1A either with or

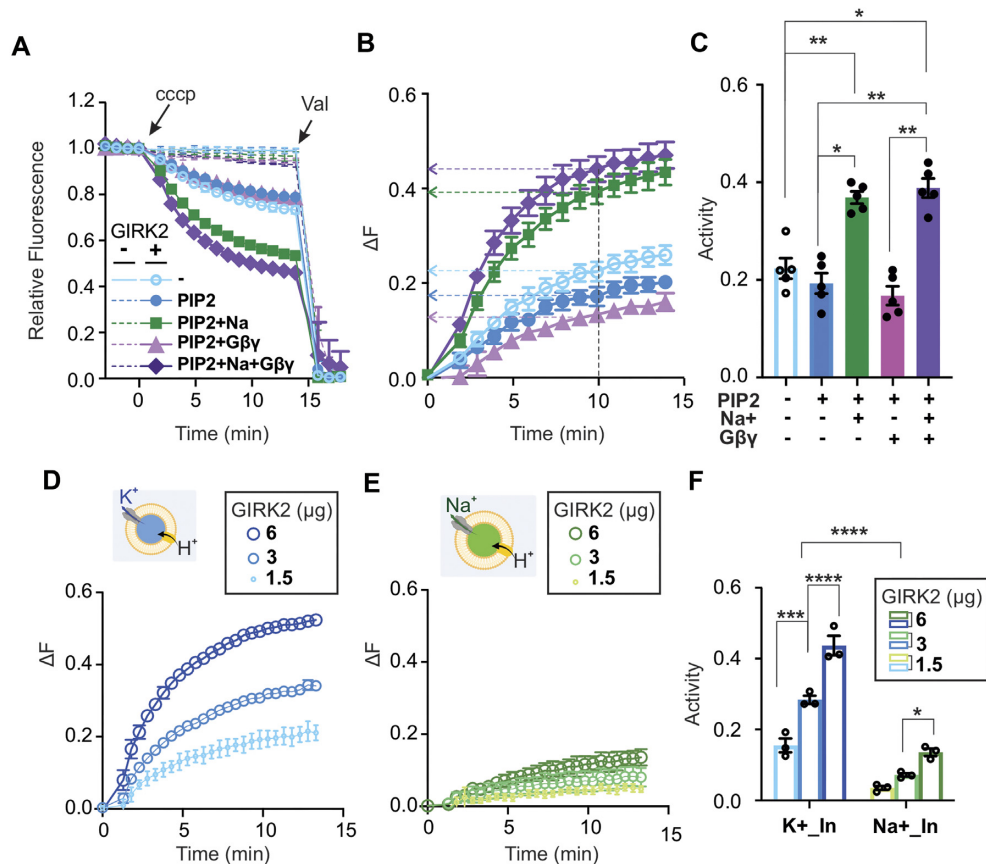


Figure 2. Canonical GIRK2 activity in reducing conditions. ACMA flux assay of reduced GIRK2 in the presence of different combinations of agonists: no agonist (cyan), PIP₂ (blue), PIP₂ + Na⁺ (green), PIP₂ + Gβγ (pink), and PIP₂ + Na⁺+Gβγ (purple). The details are in the “Method” section. (A) Representative traces of normalized fluorescence intensity for empty liposomes without proteins (dashed lines) or proteoliposomes (solid lines with marks) in the presence of different combinations of agonists. CCCP was added at 0 min, and potassium ionophore valinomycin (Val) was added at 15 min. The channel activity was inferred (C) from the differential ACMA signal decay (ΔF) between the empty liposomes and the proteoliposomes (B) at 10 min after the addition of proton ionophore (CCCP). Data are presented as the mean \pm SEM $n = 5$, and One way ANOVA followed by Tukey’s multiple comparison was used for the statistical test. No agonist vs. PIP₂ + Na, $P = .0052$; no agonist vs. PIP₂ + Na⁺+Gβγ, $P = .0164$; PIP₂ vs. PIP₂ + Na, $P = .0109$; PIP₂ vs. PIP₂ + Na⁺+Gβγ, $P = .0081$; PIP₂ + Gβγ vs. PIP₂ + Na⁺+Gβγ, $P = .0057$. Representative differential ACMA signal decay (ΔF) with increasing amount of the proteins in the absence of any agonists with internal KCl (D) or with internal NaCl (E). (F) Comparison of the basal activities measured in D and E with the internal salt K⁺ or Na⁺. Data are presented as the mean \pm SEM $n = 3$. Two-way ANOVA with Sidak’s multiple comparisons test was used for the statistical test. K⁺_In vs. Na⁺_In, $P < .001$; 3 μ g vs. 6 μ g for K⁺_In, $P = .0003$; 3 μ g vs. 6 μ g for Na⁺_In, $P = .0449$. The following color scheme is consistently applied throughout the paper. ACMA assays done with external NMDG are shown in blue colors, and those with external NaCl in green colors. Proteoliposomes containing no PIP₂ are shown in a lighter color with open symbols, and the counterparts containing PIP₂ (or PI(4)P in Figure 4) with filled symbols. Comparisons with no statistical significance are not indicated.

without added 2 mM TCEP and incubated for 30 min or 3 h at RT.

At the end of the RT incubation, the protein-lipid-detergent mix was loaded on the dehydrated Sephadex G50 column that was pre-equilibrated with the internal buffer (20 mM HEPES pH 7.5, 150 mM KCl, 0.5 mM EGTA). For experiments to test Na⁺ selectivity, 150 mM KCl of the internal buffer was replaced with 150 mM NaCl (Figure 1B), and the lipids were dissolved in the buffer containing 150 mM NaCl instead of KCl. Gβγ was added to preformed empty liposomes or proteoliposomes at 3,600 nM to make a final Gβγ concentration of 180 nM in the 200 μ L reaction volume during ACMA assays.¹⁹

A volume of 10 μ L of proteoliposome was added to each well of a 96-well plate, and then 190 μ L of the flux buffer containing 2 μ M 9-Amino-6-Chloro-2-Methoxyacridine (ACMA) in 20 mM HEPES pH 7.5, 150 mM NMDG, 0.5 mM EGTA buffer was added to get the initial base fluorescence intensity by Cytation 5 (BioTek, CA, USA) with excitation at 420 ± 20 nm and emission at 490 ± 20 nm. The flux buffer containing 150 mM NMDG was used to test GIRK2 channel activities in the absence of any

agonists as well as PIP₂ activation in the absence of coregulatory Na⁺ (Figure 1B). Flux buffer containing 150 mM NaCl instead was used to test the effect of Na⁺ on PIP₂ activation (Figure 1B). After 3 to 5 min, the proton ionophore Carbonyl Cyanide 3-ChloroPhenylhydrazide (CCCP) with 1 μ M working concentration was added to trigger proton influx down the electrical gradient generated as a result of K⁺ efflux through active channel proteins and the ACMA quenching in an activity-dependent manner. Valinomycin (if the internal salt was KCl) with 22.5 nM working concentration or monensin (if the internal salt was NaCl) with 20 nM working concentration was added 12 to 15 min after CCCP addition to trigger the maximum fluorescence decay for normalization.

The minimum fluorescence intensity after either valinomycin or monensin treatment was subtracted from all reads, and the CCCP-dependent fluorescence change expressed as a fraction of the initial fluorescence, as shown in Figure 2A. The level of channel-specific activity was then expressed as the differential fluorescence intensity ($\Delta F = F_{\emptyset} - F_p$) between empty liposomes (F_{\emptyset}) with no proteins and proteoliposomes (F_p)

(Figure 2B). For quantitative comparison, ΔF values at 10 min after CCCP were compared between different proteins and conditions (Figure 2C). All the data points were of independent samples, and none was of repeated measures of same samples.

Statistical Analysis

Statistical significance was analyzed using two-way ANOVA followed by a Šidák test for multiple comparisons using PRISM, if not otherwise stated. Statistical significance of $P < .05$, $P < .01$, $P < .001$, and $P < .0001$ is indicated by single, double, triple, and quadruple asterisks, respectively. Error bars show standard errors unless otherwise stated.

Results

Canonical GIRK2 Activity in Reducing Conditions

In intact cells, reducing conditions will normally prevail, but in our *in vitro* assays, purified proteins are vulnerable to oxidation, particularly during room temperature (RT) incubation with lipids during proteoliposome formation. Therefore, to maintain a reduced condition, reducing reagents were initially added throughout the whole purification steps as well as during the RT incubation for 3 h (see “Methods” section, Figure 1A). We then assessed activity of reduced GIRK2 channel proteins reconstituted into 1:4 POPG: POPE liposomes using the ACMA flux assay (see “Methods” section). As typically seen in cell membranes, PIP₂ led to increased channel activity in a Na⁺ and G-protein $\beta\gamma$ ($G\beta\gamma$) dependent manner^{4,22} (Figure 2A to C).

Of note is that reduced GIRK2 showed a small basal flux even in the absence of any activatory agents (Figure 2). This flux increased as the protein concentration was increased in the proteoliposomes (Figure 2D and F), and became very small when the internal salt was switched from KCl to NaCl (Figure 2E and F), indicating that it was due to K⁺ specific GIRK2 channel activity, and not to non-specific leak. Small activities observed in Figure 2E with NaCl as the internal salt were attributable to residual K⁺ ion contamination from the protein sample (Supplementary Fig. S2). Additionally, it was found that the basal activity was dependent on bulk anionic lipids (Supplementary Fig. S3). Bulk anionic lipids are essential components to maintain intact liposomes, as necessary for the ACMA assay, and practically cannot be lowered to less than 10% (w/w) for reliable results. As bulk anionic lipids were increased, basal activities increased (Supplementary Fig. S3A and B), which concomitantly decreased the channel sensitivity to Na⁺ (Supplementary Fig. S3C and D).

Anomalous GIRK2 Activity in Oxidizing Conditions

To test the effects of oxidation, proteins were purified in the absence of reducing reagents (see “Methods” section, Figure 1A). Overlapping tetramer peaks and very similar 1D SDS-PAGE bands between samples purified under reducing or oxidizing conditions indicate that GIRK2 purifies as intact tetrameric proteins in both conditions (Supplementary Fig. S1A). With the presumption that oxidation will mainly occur during incubation of the protein in lipid mix at RT, two factors, incubation time and addition of reducing agents, were varied during this step. Initially, in one batch 2 mM TCEP was added at the beginning of the incubation to prevent oxidation. GIRK2 channel activity (Figure 3A Left) then behaved essentially the same as the protein under

strictly reduced conditions (Figure 2A), at both 30-min and 3-hour incubation, indicating that there was no irreversible oxidation during the initial purification in the absence of reducing reagents.

In an initial approach to examine oxidation, protein-lipid mixtures were incubated at RT for 30 min or 3 h, without TCEP. Dramatically anomalous GIRK2 channel behaviors were then observed (Figure 3A Right). First, while basal activity of reduced proteins was stable for 3 h, basal activity of oxidized proteins was elevated after only 30-min incubation, and dramatically so after 3 h. The highly elevated basal fluxes were K⁺ specific channel fluxes since they were also proportionally increased as the protein levels increased and much smaller if the internal cation was switched to Na⁺ (Supplementary Fig. S4). Second, PIP₂ and Na⁺-dependent activation was essentially lost within 30 min RT incubation. Third, after longer incubation (3 h), rather than activating channels, PIP₂ now substantially inhibited basal activity (Figure 3B). Fourth, $G\beta\gamma$ was without effect on oxidized proteins (Figure 3C).

Given that this mild oxidative condition resulted in sufficiently slow oxidation of the channels to reveal two distinct oxidation reactions that were kinetically separable, we continued with this as a formalized approach. The differential time-dependence of the appearance of these anomalous behaviors suggests the possibility that at least two distinct oxidation events are taking place: one responsible for loss of PIP₂ and Na⁺-dependent activity, and another for elevation of basal activity. While the former was complete within 30 min, basal activity continued to increase over much longer times, suggesting that the former oxidation event more readily occurred than the latter, as we consider further below.

Nonspecific Inhibition of the Elevated Basal Activity By Phosphoinositides

Phosphoinositide activation of GIRK2 channels is not strictly limited to PIP₂ and can be supported by other PIPs including PI(5)P, PI(3,5)P₂, PI(3,4)P₂, and PI(3,4,5)P₃ but not PI(4)P²³. In order to test whether inhibition of the elevated basal activity in oxidized conditions correlated with the ability of different PIPs to activate GIRK2 under reduced conditions, a set of 3-hour RT incubation experiment was repeated in liposomes containing either PIP₂ or PI(4)P at 1% or 3%. In accordance with a previous report,²³ 1% of PI(4)P failed to activate fully reduced GIRK2 channels (Figure 4A). In contrast, both 1% of PIP₂ and (with slightly lower potency, which was not statistically significant) PI(4)P inhibited the elevated basal activity seen in the highly oxidized state (Figure 4A). Similar results were obtained with 3% PIP₂ or PI(4)P (Figure 4B), further confirming that even though PI(4)P cannot activate reduced GIRK2, both PI(4)P and PIP₂ inhibit the activity of the oxidized GIRK2.

Two Cysteine Residues Responsible for Oxidation-dependent Anomalous Activities

Although most amino acids can be oxidized under prolonged and harsh oxidative conditions,²⁴ cysteine residues are particularly susceptible.²⁵ GIRK2 has four intracellular cysteine residues; the N-terminal Cys (C65), near the PIP₂ binding site (Figure 5B orange box), is highly conserved within the Kir subfamily (Figure 5A), and a second (C190) at the bottom of the TM2 helix (Figure 5B cyan box) is conserved among Kir3 and Kir6 subfamily members (Figure 5A). We examined the consequences of

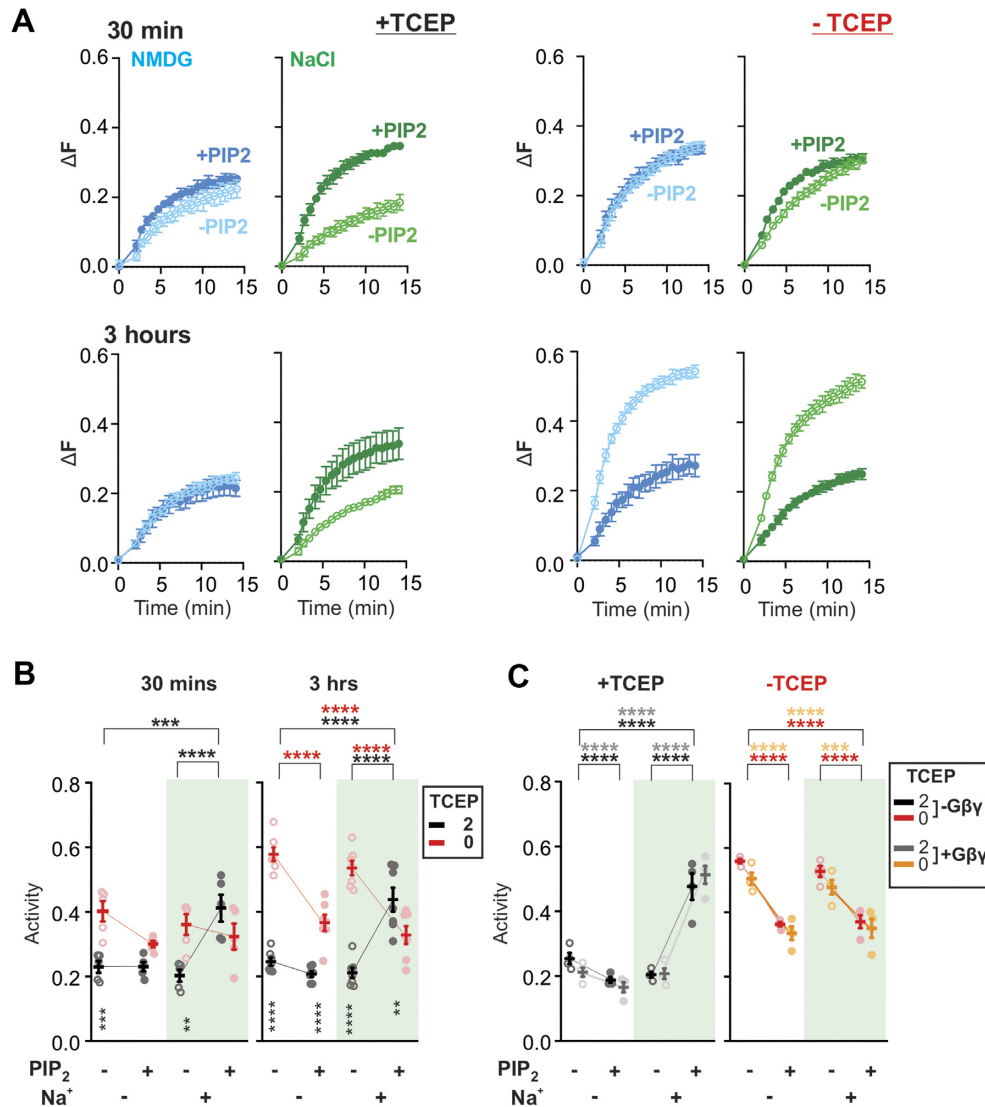


Figure 3. Anomalous GIRK2 behavior in oxidizing conditions. (A) Differential ACMA signal decay (ΔF) by GIRK2 purified without reducing reagents and incubated in reducing (+TCEP; left two columns) or oxidizing (-TCEP; right two columns) conditions for 30 min (Top) or 3 h (Bottom) at RT. Assays performed with external NMDG or Na^+ as indicated. (B) Activities either in reducing (black) or oxidizing (red) conditions are overlaid for 30-min (Left) or 3-hour (Right) incubated samples. Data are presented as the mean \pm SEM $n = 5$ in each case. Two-way ANOVA with Sidak's multiple comparisons test was used for the statistical test. Asterisks at the top of the figure indicate statistical significance between conditions as indicated. The total of 30 min + 2TCEP: no agonist vs. $\text{PIP}_2 + \text{Na}^+$, $P = .0004$; Na^+ vs. $\text{PIP}_2 + \text{Na}^+$, $P < .0001$. 3 h + 2TCEP: no agonist vs. $\text{PIP}_2 + \text{Na}^+$, $P < .0001$; Na^+ vs. $\text{PIP}_2 + \text{Na}^+$, $P < .0001$. The total of 3 h + 0TCEP: no agonist vs. PIP_2 , $P < .001$, no agonist vs. $\text{PIP}_2 + \text{Na}^+$, $P < .0001$; Na^+ vs. $\text{PIP}_2 + \text{Na}^+$, $P < .0001$. The vertically aligned asterisks indicate statistical significance for the given condition between reducing and oxidizing conditions. The total of 30 min: no agonist, $P < .0005$; Na^+ , $P = .0015$. The total of 3 h: no agonist, $P < .0001$; Na^+ , $P < .0001$; $\text{PIP}_2 + \text{Na}^+$, $P = .0054$. (C) Activities measured in the presence or absence of $G\beta\gamma$ after 3-hour RT incubation in reducing or oxidizing conditions. The activities determined with external Na^+ are shaded in green. Data are presented as the mean \pm SEM $n = 3$ in each case. Two-way ANOVA with Sidak's multiple comparisons test was used for the statistical test. Asterisks at the top of the figure indicate statistical significance between conditions as indicated. Left without $G\beta\gamma$: no agonist vs. $\text{PIP}_2 + \text{Na}^+$, $P < .0001$; Na^+ vs. $\text{PIP}_2 + \text{Na}^+$, $P < .0001$. Left with $G\beta\gamma$: no agonist vs. $\text{PIP}_2 + \text{Na}^+$, $P < .0001$; Na^+ vs. $\text{PIP}_2 + \text{Na}^+$, $P < .0001$. Right without $G\beta\gamma$: no agonist vs. PIP_2 , $P < .0001$, no agonist vs. $\text{PIP}_2 + \text{Na}^+$, $P < .0001$; Na^+ vs. $\text{PIP}_2 + \text{Na}^+$, $P < .0001$. Right with $G\beta\gamma$: no agonist vs. PIP_2 , $P < .0001$, no agonist vs. $\text{PIP}_2 + \text{Na}^+$, $P = .0001$; Na^+ vs. $\text{PIP}_2 + \text{Na}^+$, $P = .0005$.

individually mutating these two residues, as well as a double mutation of the two remaining cysteine residues (C221, C321), to oxidation-resistant amino acids (i.e., C65V, C221T/C321V, and C190S), each of which were previously shown to maintain channel activity in cellular membranes.¹⁶ Mutant channels were expressed and purified as above via two sequential size exclusion chromatography steps. All mutant proteins purified as tetramers with comparable purity to WT (Supplementary Fig. S1B and C).

The set of experiments with 3-hour RT incubation was repeated in reducing and oxidizing conditions (Figure 5C). The

behavior of the C221T/C321V double mutant was almost identical to WT, with similar oxidation-dependent and PIP_2 and Na^+ -dependent action, although PIP_2 inhibition of the oxidized protein was slightly less marked (Figure 5C). This result indicates that these two cysteines do not play critical roles in the oxidation-dependent anomalous activities. On the other hand, the C65V mutation completely abolished PIP_2 and Na^+ -dependent activation of the fully reduced protein (Figure 5C). This result indicates that C65 is normally required for PIP_2 and Na^+ -dependent GIRK2 activation and that oxidation of C65 is responsible

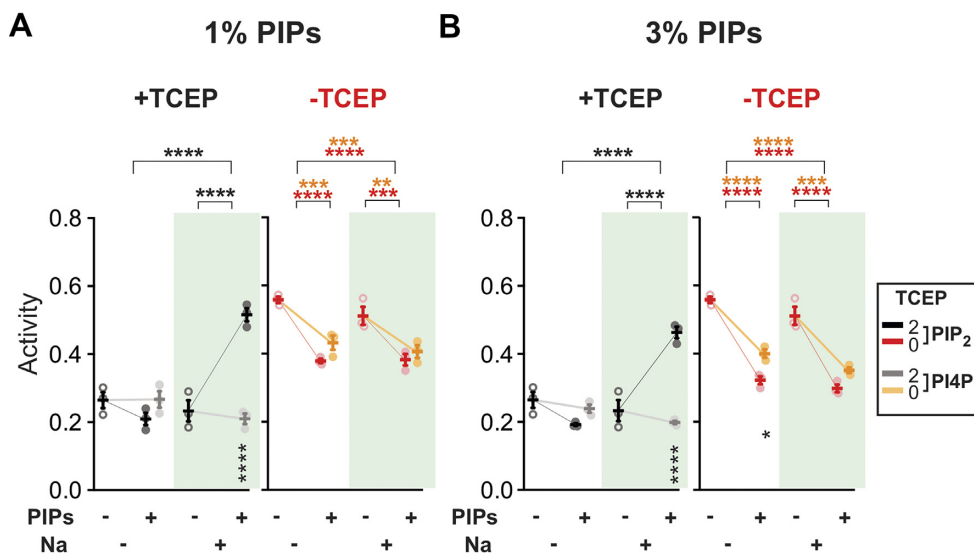


Figure 4. Nonspecific inhibition of the anomalous activity by PIPs. Activities in the presence of 1% (A) or 3% (B) PI(4)P, substituting equal amounts of PIP₂ after 3-hour RT incubation are overlaid on the Control with PIP₂, in reducing (2 mM TCEP) or oxidizing conditions, as indicated. The details are in the “Method” section. The same plotting scheme used in Figure 3C was applied. Data are presented as the mean \pm SEM $n = 3$ experiments in each condition. Two-way ANOVA with Sidak’s multiple comparisons test was used for the statistical test. Asterisks at the top of the figure indicate statistical significance between conditions as indicated. 1PIP₂ with 2 TCEP: no agonist vs. PIP₂ + Na⁺, $P < .0001$; Na⁺ vs. PIP₂ + Na⁺, $P < .0001$. 1PIP₂ with 0 TCEP: no agonist vs. PIP₂, $P < .0001$, no agonist vs. PIP₂ + Na⁺, $P < .0001$; Na⁺ vs. PIP₂ + Na⁺, $P = .0007$. 1PI(4)P with 0 TCEP: no agonist vs. PIP₂, $P = .0009$, no agonist vs. PIP₂ + Na⁺, $P = .0001$; Na⁺ vs. PIP₂ + Na⁺, $P = .0050$. 3PIP₂ with 2 TCEP: no agonist vs. PIP₂ + Na⁺, $P < .0001$; Na⁺ vs. PIP₂ + Na⁺, $P < .0001$. 3PIP₂ with 0 TCEP: no agonist vs. PIP₂, $P < .0001$, no agonist vs. PIP₂ + Na⁺, $P < .0001$; Na⁺ vs. PIP₂ + Na⁺, $P < .0001$. 3PI(4)P with 0 TCEP: no agonist vs. PIP₂, $P < .0001$, no agonist vs. PIP₂ + Na⁺, $P < .0001$; Na⁺ vs. PIP₂ + Na⁺, $P < .0001$. The vertically aligned asterisks indicate statistical significance for the given condition between PIP₂ and PI(4)P. 1PIPs with 2 TCEP: PIP₂ + Na⁺, $P < .0001$. 3PIPs with 2 TCEP: PIP₂ + Na⁺, $P < .0001$. 3PIPs with 0 TCEP: PIP₂, $P = .0116$.

for oxidation-dependent loss of PIP₂ and Na⁺-dependent activation.

Oxidation-dependent elevation of basal activity was still observed in the C65V mutant, indicating that another residue is responsible. In contrast, the reduced C190S mutant showed drastically elevated basal activity and there was no further elevation in basal activity in oxidizing conditions (Figure 5C). This implicates C190 oxidation in the elevated basal activity of oxidized WT channels. Treatment of proteoliposomes that had been kept in oxidizing conditions with DTT, a membrane permeable reducing reagent, failed to reverse the anomalous activities (Supplementary Fig. S5), indicating that the two cysteines were irreversibly oxidized in our experimental conditions.

Oxidation Influence on Kir2 Channels

In order to test whether oxidation-dependent anomalous regulation is common to other Kir channels, chicken Kir2.2 proteins were purified and functionally assessed in reducing and oxidizing conditions. Overlapping tetramer peaks and very similar 1D SDS-PAGE bands between the samples from the first (2 mM TCEP) and the second (0 mM TCEP) size exclusion step indicate that both purify as intact tetrameric proteins (Supplementary Fig. S6A). As extensively studied previously by us^{26,27} and the MacKinnon group,²⁸ reduced Kir2.2 behaves as expected (Supplementary Fig. S7A), with a very low basal activity in the absence of PIP₂ that is greatly increased by PIP₂. The same set of experiments shown in Figure 3A and B was then repeated (Figure 6A and B). PIP₂-dependent activation was lost after only 30 min of RT incubation without added TCEP (Figure 6A Right). A slight, sustained elevation of basal and K⁺ specific (Supplementary Fig. S7B) channel activity (Figure 6A) was also seen in the 0 mM TCEP condition after only 30-min incubation, although even after 3-hour RT incubation, there was neither a drastic

elevation of basal activity nor PIP₂-inhibition of basal activity.

We tested whether oxidation of a cysteine residue introduced at residue A179, equivalent to C190 of GIRK2, might also induce elevated basal activity in Kir2.2 channels. The A179C mutant protein, purified in the same manner via the two consecutive SECs, the first with and the second without TCEP, was tetrameric (Supplementary Fig. S6B), and was activated by PIP₂ if kept with added TCEP (Figure 6C). Without added TCEP, A179C also lost PIP₂ activation, but did not acquire any elevated basal activity (Figure 6C). Thus, simple introduction of cysteine at the same location did not transfer the anomalous activity observed in GIRK2 channels.

Discussion

Canonical Kir3 Channel Activity Requires Reducing Conditions

Inwardly rectifying K channels, activated by ligand interaction with muscarinic or DA receptors were first identified in cardiac atrial myocytes^{4,29} and central neurons,³⁰ close to 40 years ago. Detailed studies in the 1980s demonstrated that this activation is dependent on G-protein coupled receptor (GPCR)-released G $\beta\gamma$ subunits, which directly interact with the Kir3 (GIRK) subunits that generate these channels, at the cytoplasmic face of the membrane.⁴ Additional studies indicated that all Kir channels, including Kir3 subfamily members, normally require PIP₂ for activation,^{5,6,31} and that Kir3 subfamily members additionally require a specific interaction with cytoplasmic Na⁺ ions to facilitate this PIP₂ activation.⁸

This canonical GIRK channel gating can explain minimal basal activity and substantial activity after binding of coagonists Na⁺ and G $\beta\gamma$ ²² that is seen in intact cells. Under fully

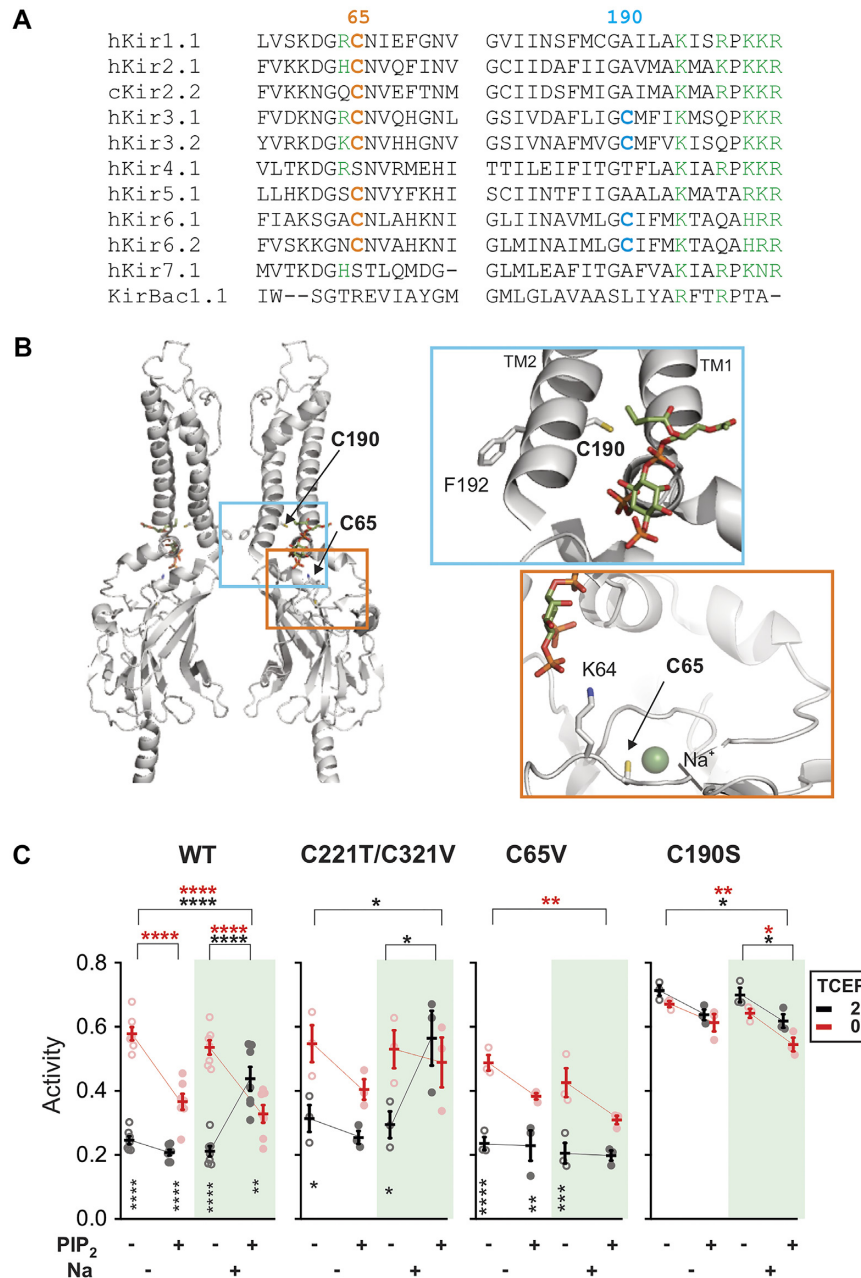


Figure 5. Cysteine knockout mutants mimicking anomalous activities. (A) Multiple Kir channel sequence alignment of the regions encompassing the first two cysteine residues of GIRK2. The conserved C65 and C190 equivalent residues are shown in orange and blue, respectively. The residues interacting with PIP₂ are shown in green. (B) Ribbon diagram of two opposing subunits of GIRK2 with zoomed in images showing the first two cysteine residues; C65 in the orange box and C190 in the cyan box. The side chains and PIP₂ are shown in sticks, Na⁺ ion is in green sphere. (C) Cys knockout mutant protein activities in the presence of different combinations of agonists, in reducing and oxidizing conditions. The same plotting scheme used in Figure 3B was applied. The graph for the wild type is the copy of Figure 3B 3-hour condition. Data are presented as the mean ± SEM *n* = 3 for all mutants. Two-way ANOVA with Sidak's multiple comparisons test was used for the statistical test. Asterisks at the top of the figure indicate statistical significance between conditions as indicated. C221TC321V with 2 TCEP: no agonist vs. PIP₂ + Na⁺, *P* = .0356; Na⁺ vs. PIP₂ + Na⁺, *P* = .0214. C65V with 0 TCEP: no agonist vs. PIP₂ + Na⁺, *P* = 0.0031. C190S with 2 TCEP: no agonist vs. PIP₂ + Na⁺, *P* = .072. C190S with 0 TCEP: no agonist vs. PIP₂ + Na⁺, *P* = .0016; Na⁺ vs. PIP₂ + Na⁺, *P* = .0142. The vertically aligned asterisks indicate statistical significance for the given condition reducing and oxidizing conditions. C221TC321V: no agonist, *P* = .0375; Na⁺, *P* = .0354. C65V: no agonist, *P* < .0001, PIP₂, *P* = .0071, Na⁺, *P* = .0003.

reduced conditions, these essential features are replicated with reconstituted GIRK protein in liposomes (Figure 2A). Basal activity observed in the absence of any agonists, in our experiments and those reported by others,^{19,20,23} is generally higher than is typically seen in unstimulated cellular conditions. One possible technical explanation is that the ACMA flux assay tends to

overestimate channel activities, since K⁺ ion efflux continues even after the Nernst potential is established, due to dissipation of the negative electric potential by proton influx through the proton ionophore, CCCP.³³ Another potential explanation is that the local environment of GIRK2 proteins in cell membranes may differ from that in recombinant liposomes; in synthetic

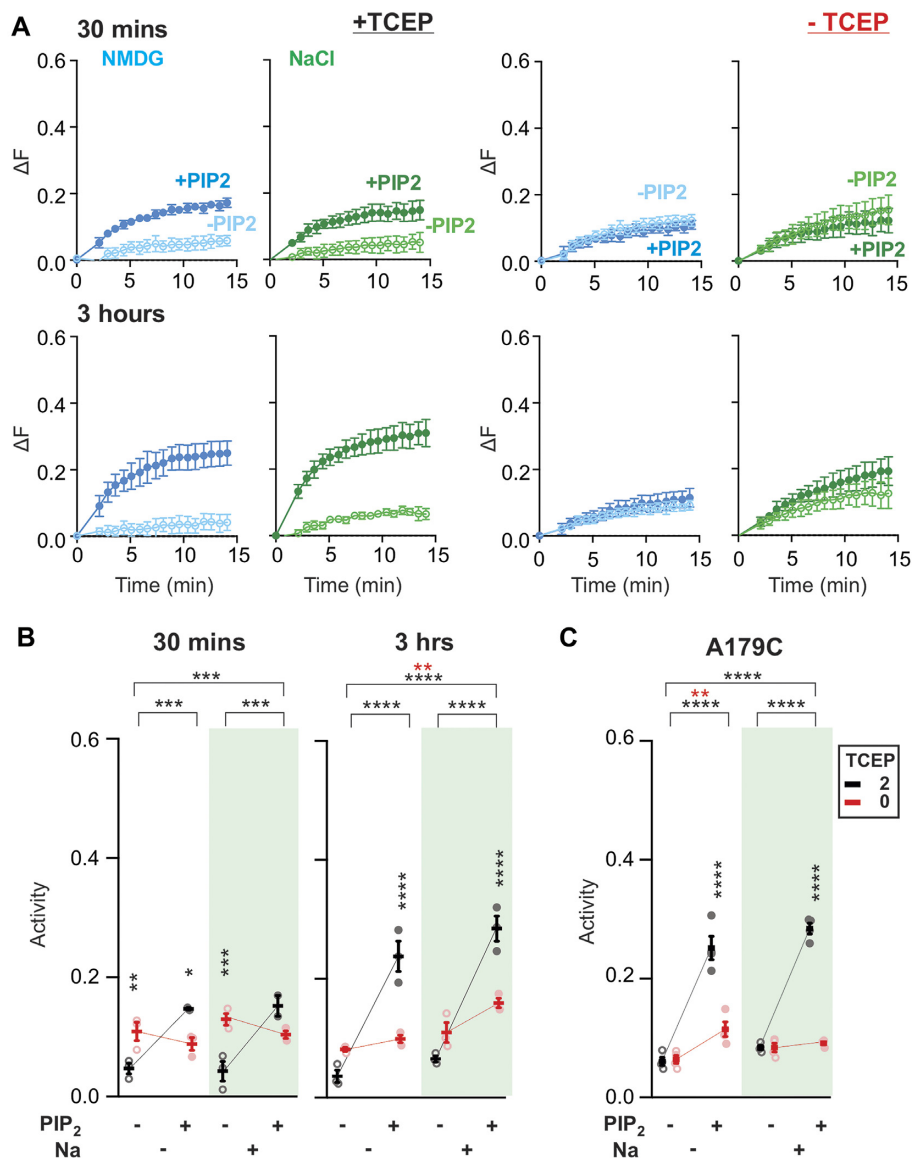


Figure 6. Oxidation dependent changes in cKir2.2 activity. (A) Differential ACMA signal decay (ΔF) due to activity of cKir2.2 purified without reducing reagents and incubated in reducing (+TCEP; Left two columns) or oxidizing (-TCEP; Right two columns) conditions for 30 min (Top) or 3 h (Bottom) at RT. (B) The activities in either reducing (black) or oxidizing (red) conditions are overlaid for 30-min (Left) or 3-hour (Right) incubated samples. Data are presented as the mean \pm SEM $n = 3$ for all mutants. Two-way ANOVA with Sidak's multiple comparisons test was used for the statistical test. Asterisks at the top of the figure indicate statistical significance between conditions as indicated. The total of 30 min with 2 TCEP: no agonist vs. PIP₂, $P = .0005$; no agonist vs. PIP₂ + Na⁺, $P = .0003$; Na⁺ vs. PIP₂ + Na⁺, $P = .0002$. The total of 3 h with 2 TCEP: no agonist vs. PIP₂, $P < .0001$; no agonist vs. PIP₂ + Na⁺, $P < .0001$; Na⁺ vs. PIP₂ + Na⁺, $P < .0001$. The total of 3 h with 0 TCEP: no agonist vs. PIP₂ + Na⁺, $P = .0081$. The vertically aligned asterisks indicate statistical significance for the given condition reducing and oxidizing conditions. The total of 30 min: no agonist, $P = .0082$; PIP₂, $P = .0251$; Na⁺, $P = .0005$. The total of 3 h: PIP₂, $P < .0001$; PIP₂ + Na⁺, $P < .0001$. (C) The activities of cKir2.2 A179C protein purified without reducing reagents after 3-hour incubation in reducing (black) or oxidizing (red) conditions. The same plotting scheme used in Figure 3B was applied. Data are presented as the mean \pm SEM $n = 4$ for all mutants. Two-way ANOVA with Sidak's multiple comparisons test was used for the statistical test. Asterisks at the top of the figure indicate statistical significance between conditions as indicated. Two TCEP: no agonist vs. PIP₂, $P < .0001$; no agonist vs. PIP₂ + Na⁺, $P < .0001$; Na⁺ vs. PIP₂ + Na⁺, $P < .0001$. 0 TCEP: no agonist vs. PIP₂, $P = .0083$. The vertically aligned asterisks indicate statistical significance for the given condition reducing and oxidizing conditions. PIP₂, $P < .0001$; PIP₂ + Na⁺, $P < .0001$.

membranes, GIRK2 proteins are sparsely distributed, and in the absence of cytoskeletal or other associated proteins. In addition, the liposomes contain significant [20 (w/w) %] anionic lipids (POPG), necessary to create tight liposomes. These bulk anionic lipids themselves elevated basal activity (Supplementary Fig. S3), and it is possible that local anionic lipid levels near GIRK channels in native membranes GIRK2 proteins are much lower than the measured average content of ~10% to 15%. Finally,

considering the inhibitory effect of some PIPs (Figure 4),²³ the absence of these lipids in our proteoliposomes may also contribute to the emergence of basal activities. Interestingly opening of Kir6.2 channels in synthetic membranes without PIP₂ was recently reported.³⁴ Considering that among the Kir subfamilies, the highest sequence similarity is between Kir3 (GIRK) and Kir6 subfamilies, this basal activity in the absence of PIP₂ may arise from common amino acid compositions that are unique to these

two subfamilies. This may explain why the Kir2.2 A179C mutant did not acquire elevated basal activity after 3-hour RT incubation in the absence of TCEP (Figure 6C).

Reversed Gating Upon Oxidation: Molecular Basis

The present study provides a straightforward explanation for the canonical behavior of GIRK channels in intact cells as reflecting the behavior of fully reduced proteins within the normal intracellular milieu, but with emergence of noncanonical behaviors, reflecting the consequences of protein purification, in oxidizing conditions. Striking changes in gating of GIRK2 channels in the oxidative condition are the dramatic increase in ligand-independent, but K^+ -selective, channel activity, alongside a complete loss of PIP_2 , and Na^+ -dependent activation (Figure 3). That these two consequences result from distinct oxidation events are suggested by their temporal separation: PIP_2 and Na^+ -dependent activation is lost within 30 min but increase of basal activity continues for a few hours under our experimental conditions. While we cannot formally exclude any potential roles of lipid oxidation, the mutational effects of two specific cysteines argues that oxidation of these cysteines are the key determinants. The C65V mutation completely abolished PIP_2 activation, even under fully reduced conditions. This implicates C65 oxidation as being responsible for the rapid loss of PIP_2 and Na^+ -dependent activation and is consistent with previous studies that reported loss of cellular GIRK2 activity when this cysteine residue is mutated to various other amino acids or otherwise modified.^{13,16,35–37} The molecular mechanism for the loss of PIP_2 and Na^+ -dependent activation is yet to be determined; the mutation may abolish PIP_2 binding or prevent conformational change required for PIP_2 binding, or for transduction from binding to channel opening. However, given the robust PIP_2 inhibition effect on oxidized proteins, the latter seems most likely, and our gating model is in line with this mechanism. Interestingly, in the recent cryo EM structure of GIRK2 determined in complex with PIP_2 but in the absence of Na^+ (6XIT),³⁸ the C65 side chain is facing up toward the transmembrane domain while the side chain faces the interior of the cytoplasmic domain (CTD) in three other crystal structures determined in the presence of Na^+ (Figure 7A). This unique side chain orientation in the 6XIT structure is accompanied by an unstructured βA strand that no longer forms a β sheet with βL and βM strands from the neighboring subunit. It is possible that the oxidized C65 sidechain may adopt the vertically oriented conformation seen in 6XIT, and that attenuated inter-subunit coupling ablates the conformational changes in the CTD upon binding of agonists.

Alignment of the relevant primary sequences of GIRK channels and other eukaryotic and prokaryotic Kir channels (Figure 5A) shows that residue C65 is highly conserved, and hence likely to be critical for channel function, throughout the eukaryotic Kir channel family. Consistent with this, oxidized Kir2.2 also lost PIP_2 activation in our in vitro assay (Figure 6). Sulfhydryl modification of the C65 equivalent residue reportedly decreased Kir2.3³⁸ and Kir6.2³⁹ channel activity, but increased Kir6.1 channel activity,⁴⁰ although in the latter cases it is unclear whether confounding effects on intrinsic open probability, or on inhibitory ATP sensitivity could be involved.

The C190S mutation increased the basal activity of oxidized or reduced GIRK2 to maximal levels (Figure 5C), supporting C190 oxidation as being responsible for elevated basal activity of the oxidized protein, with the slow kinetics of this oxidization effect potentially being explained by limited solvent accessibility of

this residue. Cysteine at the equivalent residue is conserved only between Kir3 (GIRK) and Kir6 sub-families (Figure 5A). Consistent with cysteine oxidation specifically being required for this activation, mutation of C190 to multiple other amino acids (Thr, Ile, Val, Ala, Gln, and Met) has been shown to render GIRK channels constitutively active and less responsive to G protein activation.⁴¹ In Kir6.x channels, mutations of the equivalent residue (C166 in Kir6.2, C176 in Kir6.1) also leads to a markedly elevated intrinsic open probability and consequently reduced ATP inhibitory sensitivity,^{42,43} causing the monogenic diseases neonatal diabetes⁴⁴ and Cantu syndrome.⁴⁵ Modification by a palmitoyl moiety or sulfhydryl groups also markedly affects channel function.^{36,46,47} However, a simple introduction of the equivalent cysteine to the Kir2.2 channel (A179C mutation) failed to transfer oxidation-induced elevated basal activity (Figure 6C), indicating that whole protein architecture is important for this anomalous activation, rather than simply local chemistry changes.

An intriguing observation in our study is that the elevated basal activity is inhibited by PIP_2 (Figure 3). GIRK2 channel activation is not strictly PIP_2 specific, and other PIPs are also activatory but less effective than PIP_2 .²⁴ While PI(4)P failed to activate GIRK2 (Figure 4), in accordance with a previous report,²³ it inhibited the basal activity of oxidized GIRK2 as effectively as PIP_2 , suggesting both PI(4)P and PIP_2 stabilize the same conformation that leads to reduction in basal activity. This raises the possibility that PI(4)P may also bind to reduced GIRK proteins just as PIP_2 does but fail to trigger the additional conformational change(s) that are normally induced by PIP_2 in conjunction with Na^+ and $G\beta\gamma$ to open the channel. How PI(4)P incapable of activating GIRK2 but capable of inhibiting the elevated basal activity is discussed below.

Close examination of C190 residue and its surroundings in the available structures reveals that the C190 thiol group gets closer to the backbone amide of V87 as the proteins bind more activatory ligands (Figure 7B). The C190S mutation, or oxidation of C190 to sulfinic or sulfonic acid, may then facilitate interaction with the slide helix and hence increase open state stability.

How Does Oxidation Happen?

The most likely source of the oxidative stress is molecular oxygen dissolved into the samples from the air. Spontaneous autoxidation of thiols by molecular oxygen of cysteine side chains can occur in the absence of enzymes or radical initiators such as peroxides, but reaction rates are generally low at neutral pH and low temperatures.^{48,49} However, transition metals can generate both hydrogen peroxide and superoxide when encountered molecular oxygen,⁵⁰ accelerating the autoxidation of cysteine.^{49,51} Thus, it seems likely that transition metals included in our buffers as contaminants might have generated initial reactive oxygen species (ROS). Also, as discussed previously by Zeidner and colleagues,¹⁵ C65 is highly reactive and becomes ionized to S^- with the negatively charged state stabilized by the neighboring lysine (K64).^{52,53} Subsequent chain reactions can occur to reversibly oxidize the thiol group of cysteine sidechains to sulfenyl acid, but this unstable moiety is then rapidly converted to irreversible and stable sulfinic and sulfonyl acid.⁵⁴ While, the exact species of the oxidized cysteines are yet to be determined, the oxidized cysteines in our experiments were insensitive to DTT treatment (Supplementary Fig. S5), suggesting they were in stable irreversible forms.

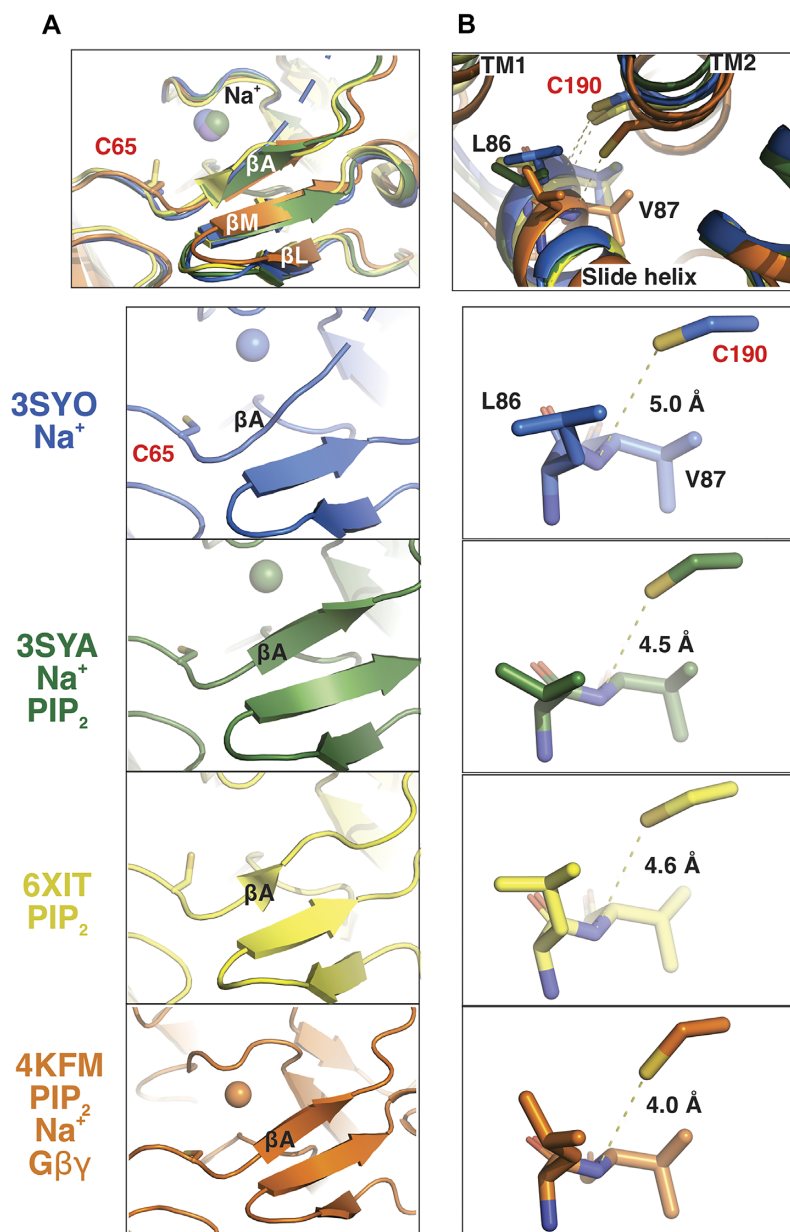


Figure 7. Local GIRK2 structures near C65 and C190. Three crystal and a cryo EM structures of GIRK2 wildtype are shown in ribbon diagrams and colored in blue for 3SYO in complex with Na⁺, green for 3SYA in complex with PIP₂ + Na⁺, and yellow for 6XIT in complex with PIP₂, and orange for 4KFM in complex with PIP₂ + Na⁺ + Gβγ. (A) The region near C65 residue is zoomed in, Na⁺ ions are shown in spheres, and the secondary structures of neighboring parts are shown for comparison. (B) The region near C190 residue is zoomed in, and C190 and the residues close to C190 side chain are shown in sticks. The distance between the thiol group of C190 side chain and the nitrogen atom of V87 amine group is measured.

Gating Model of Reduced and Oxidized GIRK Channels

Both the helix-bundle crossing (HBC) at the bottom of the transmembrane domain (TMD) and the G-loop at the apex of the C-terminal cytoplasmic domain (CTD) have been implicated as locations of gating in GIRK and other Kir channels.^{18,19,38,55} A recent single particle Cryo-EM study showed that the binding of PIP₂, even in the absence of Na⁺ or Gβγ, widened the HBC but constricted the G-loop in GIRK2 via a clockwise rotational/twisting motion in the CTDs of the PIP₂-bound (PDB:6XIT) structure, as the CTD became tightly engaged with the TMD.³⁸ Notably, the recent Cryo-EM structure of the highly active Kir6.2 C166S/G334D mutant was determined in a clearly open state

in the absence of PIP₂.³⁵ Given that the C166S mutation of Kir6.2 is equivalent to C190S of GIRK2, it seems likely that GIRK2 C190S may adopt a similar open state structure in the absence of PIP₂. With this as an assumption, alignment of the PIP₂-bound GIRK2 EM structure (6XIT) and PIP₂-unbound Kir6.2 C166S/G334D EM structure (7S5T) at the TM helices, suggests a rotational/twisting motion of GIRK2 in a clockwise direction that constricts the G-loop gate (Figure 8A Left), relative to the PIP₂-unbound Kir6.2 C166S/G334D. Molecular dynamics simulations of GIRK2 channels in the presence of PIP₂ also indicate that PIP₂ binding leads to widening of the HBC gate but narrowing of the G-loop gate.^{56,57} These observations together suggest

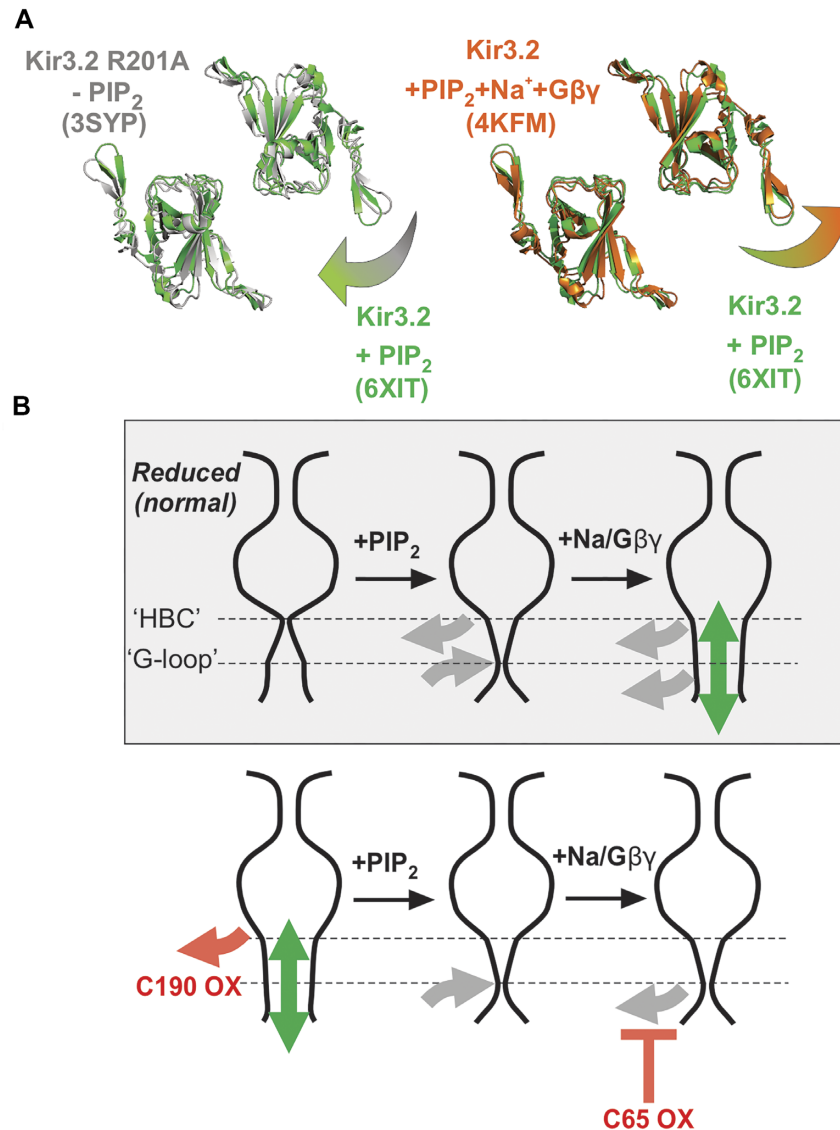


Figure 8. Proposed GIRK2 gating model. (A) CTD conformational changes induced in the presence of different ligands. (Left) Overlaid ribbon diagrams (viewed through the membrane looking into the cytoplasm) of two opposing CTDs of GIRK2 cryo EM structure in complex with PIP₂ (PIP₂-bound: 6XIT) in green and of Kir6.2 C166S/G334D cryo EM structure in the absence of PIP₂ (PIP₂-unbound: 7S5T). (Right) Overlaid ribbon diagrams of the same two opposing CTDs of GIRK2 in complex with PIP₂ (PIP₂-bound: 6XIT) in green or in complex with PIP₂, Na⁺, and Gβγ (Holo:4KFM) in orange. The arrows indicate rotational/twisting motions of the CTD induce by binding of either PIP₂ alone (Left) or PIP₂ plus Na⁺ and Gβγ (Right); clockwise motion narrows but counterclockwise motion widens the G-loop gate. (B) GIRK2 gating models. Top: canonical GIRK2 gating in the reduced state. In the Apo state, the HBC gate is closed while the G-loop gate is open. PIP₂ opens the HBC gate but the induced clockwise rotational/twisting motions of the CTD close the G-loop gate. The additional binding of positive cofactors, Na⁺ and/or Gβγ, makes the channel conductive by triggering counterclockwise rotational/twisting motions in the CTD, and opening of the G-loop gate. (Bottom) Proposed gating alterations resulting from oxidation. Oxidation of C190 opens the HBC gate in the absence of any ligands, resulting in open channels. PIP₂ binding still closes the G-loop gate, inhibiting the basal activity. Oxidation of C65 prevents the action of the two cofactors, Na⁺ and/or Gβγ, resulting in loss of PIP₂ and Na⁺-dependent activation, potentially by preventing the necessary counterclockwise rotation/twisting motion in the CTD.

a structural reason why PIP₂ by itself is incapable of activating GIRK channels.^{9,58} In simulations, the G-loop was only widened after Na⁺ and/or Gβγ were included in the simulations.⁵⁶ The G-loop gate was also slightly wider in the GIRK2 holo-crystal structure complexed with PIP₂, Na⁺, and Gβγ (PDG:4KFM),¹⁹ accompanied by a counterclockwise rotational/twisting motion of the CTD, compared to the PIP₂-only bound GIRK2 EM structure³⁸ as reported previously¹⁹ (Figure 8A Right). Although quite subtle, these structural changes could be much more pronounced in solution and at higher temperature, as was the case for the HBC gate, which opened widely during MD simulations.⁵⁷

These studies lead us to propose the following gating model for GIRK channels that provides an explanatory framework for how oxidation modifies normal gating, resulting in the observed anomalous activities (Figure 8B). In the absence of agonists, in the normal reduced state, the HBC gate is closed, and the G-loop gate is open. PIP₂ binding has two opposite effects on these gates; PIP₂ opens the HBC gate but closes the G-loop gate. Hence, the channel remains functionally closed in this condition. When Na⁺ and/or Gβγ are bound, additional conformational changes, potentially the result of counterclockwise rotation/twisting motions in the CTDs, cause opening of the G-loop gate and make the channel conductive (Figure 8B Top).

Oxidation can alter this normal gating in two stages (Figure 8B Bottom). Oxidation of C65 is proposed to prevent the CTD conformational change and G-loop opening that results from binding of Na⁺ and/or Gβγ, and hence leads to complete loss of PIP₂ and Na⁺-dependent activation. Conversely, we propose that C190 oxidation opens the HBC gate in the absence of PIP₂. With both HBC and G-loop gates open, the channels are then highly active under basal conditions. PIP₂ binding to the channel with oxidized C190 (mimicked by mutation C190S, Figure 5) will still close the G-loop gate and hence reduces channel activity, whether or not C65 is also oxidized.

Unlike PIP₂, PI(4)P is not proposed to induce the conformational changes in the CTD that open the G-loop gate. Hence, PI(4)P cannot activate GIRK2 channels but rather can only inhibit basal activities by constricting the G-loop gate (Figure 4).

Finally, although it is understood that the activity of all eukaryotic Kir channels is normally activated by interaction with PIP₂, a long-standing and unexplained finding is that reconstituted prokaryotic KirBac1.1 channels are spontaneously active, and strongly inhibited by PIP₂,⁵⁹ paralleling the behavior of oxidized GIRK2 channels. Thus, gating of KirBac1.1 could be explained if this cysteine-less channel also has open HBC and G-loop gates in the absence of PIP₂, with the G-loop gate also being closed by the binding of PIP₂. Consistent with this suggestion, PIP₂ binding to KirBac1.1 does constrict the G-loop region.⁶⁰ Further structural studies are needed, but this attractively simple hypothesis may well explain this long-held mystery of reversed gating in prokaryotic and eukaryotic Kir channels.

Reversed Gating Upon Oxidation: Reconciling Previous Contradicting Observations

There have been contradicting reports regarding GIRK channel modulation by oxidative stresses and none have drawn a link between oxidation in vitro and the aberrant behaviors observed in recombinant channels. One study showed that GIRK channel activity was elevated, in a Gβγ-independent manner, by exposure to the cell-permeable reducing agent dithiothreitol (DTT).¹⁵ Inhibition of GIRK channel activity due to reversible oxidation was also reported in a separate study.¹⁶ On the other hand, Jeglitsch et al.¹⁷ reported the discordant observation that exogenous free radical treatment triggered transient GIRK activation, also in a Gβγ-independent manner. Our work now provides a molecular mechanistic explanation for these contradicting observations. Even in normal physiological conditions, a subset of reactive C65 residues are likely to become oxidized and form mixed disulfides with small anti-oxidant molecules such as s-glutathione, and become inactive due to loss of PIP₂ sensitivity, such that reversal by DTT treatment could result in augmented activity. In the latter case,¹⁷ xanthine oxidase can generate superoxide anions (O₂^{•-}) and hydrogen peroxide (H₂O₂) in the extracellular side.⁶¹ These ROS can cross the cell membrane both via membrane proteins such as aquaporin and chloride channels,⁶² or via simple diffusion through the membrane at fairly low rates (4.4x e⁻⁴ cm/s for H₂O₂ and 2.1x e⁻⁶ cm/s for O₂^{•-}).^{63,64} It is conceivable that slow diffusion of these ROS across the plasma membrane may then oxidize C190, buried in the hydrophobic interior of the membrane, which could increase channel activity to levels observed for the C190S mutant in cell membranes.⁶⁵

Reversed Gating Upon Oxidation: Pathophysiological Implications

Our results show that oxidation is a functionally relevant modulatory factor that can have a strong effect on GIRK channel activity. Under oxidatively stressed conditions, this could cause rapid decrease of cellular GIRK activity via C65 oxidation while, potentially, extended oxidative stresses could additionally oxidize residue C190 and constitutively activate GIRK channels. Conceivably, oxidation-driven closure of GIRK channels, by depolarizing cells, could be a powerful promoter of apoptotic cell death⁶⁶ in general. By attenuating GIRK channel function, modification of residue C65 by the metabolized prodrug (L-DOPA), a treatment for PD, can cause loss of dopaminergic neurons and eventually exacerbation of PD after long-term use of the drug.¹³ Conversely, pathologies that may be linked to hyperactive GIRK channels under oxidative stress conditions have also been identified. Hyperactivity of Kir3 (GIRK) channels has been implicated in dilation of renal afferent arterioles of rats with type 1 diabetes mellitus (T1D).⁶⁷ The dilation was diminished if rats were pretreated with Tempol, a membrane-permeable antioxidant, consistent with oxidation as the cause of the elevated GIRK activity.⁶⁸ In addition, Kir3-dependent muscarinic-activated currents (I_{KACH}) are functionally upregulated during chronic atrial fibrillation (cAF).⁶⁹ While uncontrolled phosphorylation has been identified as partly responsible for constitutive, PIP₂- and Na⁺-independent, channel activity in cAF,⁷⁰ chronic ROS elevation is also one of the key understood drivers of cardiac remodeling in the development of cAF,^{71,72} and it is also possible that direct oxidation of GIRK channels at the C190 residue is at fault.

Acknowledgments

We thank Dr. Rodrick Mackinnon for kindly sharing the Kir3.2 clone for expression in *Pichia Pastoris*. This work was supported by CIMED Pilot and Feasibility grant CIMED-21-02 and NIH R03 grant TR003670 (to SJL), and NIH R35 grant HL140024 (to CGN).

Author contributions

S.J.L. conceived the project. S.J.L., S.M., and J.G. carried out experiments, and S.J.L. analyzed the data. S.J.L. and C.G.N. wrote the manuscript, which was edited by S.M. and J.G.

Supplementary Material

Supplementary material is available at the APS Function online.

Conflicts of interests

The authors declare no conflict of interest. Colin G. Nichols holds the position of Executive Editor for Function and is blinded from reviewing or making decisions for the manuscript.

Data Availability

The authors declare that the data underlying the findings of this study are available within the paper and its Supplementary Information files are available upon request.

References

- Hibino H, Inanobe A, Furutani K, Murakami S, Findlay I, Kurachi Y Inwardly rectifying potassium channels: their

- structure, function, and physiological roles. *Physiol Rev.* 2010;**90**(1): 291–366.
- 2 Kaupmann K, et al. Human gamma-aminobutyric acid type B receptors are differentially expressed and regulate inwardly rectifying K⁺ channels. *Proc Natl Acad Sci USA.* 1998; **95**(25): 14991–14996.
 - 3 Werner P, Hussy N, Buell G, Jones KA, North R A. D2, D3, and D4 dopamine receptors couple to G protein-regulated potassium channels in *Xenopus* oocytes. *Mol Pharmacol.* 1996; **49**(4): 656–661.
 - 4 Logothetis DE, Kurachi Y, Galper J, Neer EJ, Clapham DE The beta gamma subunits of GTP-binding proteins activate the muscarinic K⁺ channel in heart. *Nature.* 1987; **325**(6102): 321–326.
 - 5 Huang CL, Feng S, Hilgemann DW Direct activation of inward rectifier potassium channels by PIP2 and its stabilization by Gbetagamma. *Nature.* 1998; **391**(6669): 803–806.
 - 6 Sui JL, Petit-Jacques J, Logothetis DE. Activation of the atrial K⁺ channel by the betagamma subunits of G proteins or intracellular Na⁺ ions depends on the presence of phosphatidylinositol phosphates. *Proc Natl Acad Sci USA.* 1998; **95**(3): 1307–1312.
 - 7 Kobayashi T, et al. Ethanol opens G-protein-activated inwardly rectifying K⁺ channels. *Nat Neurosci.* 1999; **2**(12): 1091–1097.
 - 8 Petit-Jacques J, Sui JL, Logothetis DE Synergistic activation of G protein-gated inwardly rectifying potassium channels by the betagamma subunits of G proteins and Na⁺ and Mg²⁺ ions. *J Gen Physiol.* 1999; **114**(5): 673–684.
 - 9 Sui JL, Chan KW, Logothetis DE Na⁺ activation of the muscarinic K⁺ channel by a G-protein-independent mechanism. *J Gen Physiol.* 1996; **108**(5): 381–391.
 - 10 Wang W, Whorton MR, MacKinnon R Quantitative analysis of mammalian GIRK2 channel regulation by G proteins, the signaling lipid PIP2 and Na⁺ in a reconstituted system. *Elife.* 2014; **3**:e03671.
 - 11 Beaulieu JM, Gainetdinov RR The physiology, signaling, and pharmacology of dopamine receptors. *Pharmacol Rev.* 2011; **63**(1): 182–217.
 - 12 Ebadi M, et al. Metallothionein-mediated neuroprotection in genetically engineered mouse models of Parkinson's disease. *Brain Res Mol Brain Res.* 2005; **134**(1): 67–75.
 - 13 Bizzarri BM, Botta L, Aversa D, et al. L-DOPA-quinone mediated recovery from GIRK channel firing inhibition in dopaminergic neurons. *ACS Med Chem Lett.* 2019; **10**(4): 431–436.
 - 14 Lipski J, et al. L-DOPA: a Scapegoat for accelerated neurodegeneration in Parkinson's disease? *Prog Neurobiol.* 2011; **94**(4): 389–407.
 - 15 Zeidner G, Sadjia R, Reuveny E Redox-dependent gating of G protein-coupled inwardly rectifying K⁺ channels. *J Biol Chem.* 2001; **276**(38): 35564–35570.
 - 16 Guo Y, Waldron GJ, Murrell-Lagnado R A role for the middle C terminus of G-protein-activated inward rectifier potassium channels in regulating gating. *J Biol Chem.* 2002; **277**(50): 48289–48294.
 - 17 Jeglitsch G, et al. The cardiac acetylcholine-activated, inwardly rectifying K⁺-channel subunit GIRK1 gives rise to an inward current induced by free oxygen radicals. *Free Radic Biol Med.* 1999; **26**(3–4): 253–259.
 - 18 Whorton, Matthew R, MacKinnon R Crystal structure of the mammalian GIRK2 K⁺ channel and gating regulation by G proteins, PIP2, and sodium. *Cell.* 2011;**147**(1): 199–208.
 - 19 Whorton MR, MacKinnon R X-ray structure of the mammalian GIRK2-[bgr][ggr] G-protein complex. *Nature.* 2013; **498**: 190–197.
 - 20 Glaaser IW, Slesinger PA Dual activation of neuronal G protein-gated inwardly rectifying potassium (GIRK) channels by cholesterol and alcohol. *Sci Rep.* 2017; **7**(1): 4592.
 - 21 Wang W, Touhara KK, Weir K, Bean BP, MacKinnon R Cooperative regulation by G proteins and Na⁺ of neuronal GIRK2 K⁺ channels. *Elife.* 2016;**5**: e15751.
 - 22 Hilger D, et al. Structural insights into differences in G protein activation by family A and family B gpcrs. *GPCRs.* *Science.* 2020; **369**:eaba3373.
 - 23 Reuveny E, et al. Activation of the cloned muscarinic potassium channel by G protein beta gamma subunits. *Nature.* 1994; **370**(6485):143–146.
 - 24 Lacin E, Aryal P, Glaaser IW, et al. Dynamic role of the tether helix in PIP. *J Gen Physiol.* 2017; **149**(8): 799–811.
 - 25 Davies MJ The oxidative environment and protein damage. *Biochim Biophys Acta.* 2005; **1703**(2): 93–109.
 - 26 Gupta V, Carroll KS Sulfenic acid chemistry, detection and cellular lifetime. *Biochim Biophys Acta.* 2014; **1840**(2): 847–875.
 - 27 Lee SJ, et al. Secondary anionic phospholipid binding site and gating mechanism in Kir2.1 inward rectifier channels. *Nat Commun.* 2013; **4**(1): 2786.
 - 28 Lee SJ, et al. Structural basis of control of inward rectifier Kir2 channel gating by bulk anionic phospholipids. *J Gen Physiol.* 2016; **148**(3): 227–237.
 - 29 Hansen SB, Tao X, Mackinnon R Structural basis of PIP2 activation of the classical inward rectifier K⁺ channel Kir2.2. *Nature.* 2011; **477**(7365): 495–498.
 - 30 Sakmann B, Noma A, Trautwein W Acetylcholine activation of single muscarinic K⁺ channels in isolated pacemaker cells of the mammalian heart. *Nature.* 1983; **303**(5914): 250–253.
 - 31 Gähwiler BH, Brown DA GABAB-receptor-activated K⁺ current in voltage-clamped CA3 pyramidal cells in hippocampal cultures. *Proc Natl Acad Sci USA.* 1985; **82**(5): 1558–1562.
 - 32 Hilgemann DW, Ball R Regulation of cardiac Na⁺,Ca²⁺ exchange and K_{ATP} potassium channels by PIP₂. *Science.* 1996; **273**(5277): 956–959.
 - 33 Lee SY, Letts JA, MacKinnon R Functional reconstitution of purified human Hv1 H⁺ channels. *J Mol Biol.* 2009; **387**(5): 1055–1060.
 - 34 Lemmon MA Membrane recognition by phospholipid-binding domains. *Nat Rev Mol Cell Biol* 2008; **9**(2): 99–111.
 - 35 Zhao C, MacKinnon R Molecular structure of an open human KATP channel. *PNAS* 2021;**118**(48):e2112267118
 - 36 Inanobe A, Matsuura T, Nakagawa A, Kurachi Y Inverse agonist-like action of cadmium on G-protein-gated inward-rectifier K⁺ channels. *Biochem Biophys Res Commun* 2011; **407**(2): 366–371.
 - 37 Yang Y, et al. Molecular basis and structural insight of vascular K_{ATP} channel gating by S-glutathionylation. *J Biol Chem* 2011; **286**(11): 9298–9307.
 - 38 Ha J, et al. Hydrogen sulfide inhibits Kir2 and Kir3 channels by decreasing sensitivity to the phospholipid phosphatidylinositol 4,5-bisphosphate (PIP₂). *J Biol Chem* 2018; **293**(10): 3546–3561.
 - 39 Niu Y, Tao X, Touhara KK, MacKinnon R Cryo-EM analysis of PIP₂ regulation in mammalian GIRK channels. *Elife* 2020; **9**: e60552.
 - 40 Tucker SJ, et al. Molecular determinants of KATP channel inhibition by ATP. *EMBO J* 1998; **17**(12): 3290–3296.

- 41 Mustafa AK, et al. Hydrogen sulfide as endothelium-derived hyperpolarizing factor sulfhydrates potassium channels. *Circ Res* 2011; **109**(11): 1259–1268.
- 42 Sadjja R, Smadja K, Alagem N, Reuveny E Coupling gbetagamma-dependent activation to channel opening via pore elements in inwardly rectifying potassium channels. *Neuron* 2001; **29**(3): 669–680.
- 43 Trapp S, Proks P, Tucker SJ, Ashcroft FM. Molecular analysis of ATP-sensitive K channel gating and implications for channel inhibition by ATP. *J Gen Physiol* 1998; **112**(3): 333–349.
- 44 Enkvetchakul D, Loussouarn G, Makhina E, Shyng SL, Nichols CG. The kinetic and physical basis of K(ATP) channel gating: toward A unified molecular understanding. *Biophys J* 2000; **78**(5): 2334–2348.
- 45 Gloy AL, Diatloff-Zito C, Edghill EL, et al. KCNJ11 activating mutations are associated with developmental delay, epilepsy and neonatal diabetes syndrome and other neurological features. *Eur J Hum Genet* 2006; **14**(7): 824–830.
- 46 Cooper PE, et al. Cantú syndrome resulting from activating mutation in the KCNJ8 gene. *Hum Mutat* 2014; **35**(7): 809–813.
- 47 Yang HQ, et al. Palmitoylation of the KATP channel Kir6.2 subunit promotes channel opening by regulating PIP2 sensitivity. *Proc Natl Acad Sci USA* 2020; **117**(19): 10593–10602.
- 48 Yang Y, Shi W, Cui N, Wu Z, Jiang C Oxidative stress inhibits vascular K_{ATP} channels by S-glutathionylation. *J Biol Chem* 2010; **285**(49): 38641–38648.
- 49 Wallace TJ, Schriesheim A. The base-catalysed oxidation of aliphatic and aromatic thiols and disulphides to sulphonic acids. *Tetrahedron* 1965; **21**(9): 2271–2280.
- 50 Bagiyana GA, Koroleva IK, Soroka NV, Ufimtse AV Oxidation of thiol compounds by molecular oxygen in aqueous solutions. *Russ Chem Bull* 2003; **52**: 1135–1141.
- 51 Nath KA, Salahudeen AK Autoxidation of cysteine generates hydrogen peroxide: cytotoxicity and attenuation by pyruvate. *Am J Physiol* 1993; **264**(2): F306–314.
- 52 Wang XF, Cynader MS Pyruvate released by astrocytes protects neurons from copper-catalyzed cysteine neurotoxicity. *J Neurosci* 2001; **21**(10): 3322–3331.
- 53 Zheng M, Aslund F, Storz G Activation of the OxyR transcription factor by reversible disulfide bond formation. *Science* 1998; **279**(5357): 1718–1721.
- 54 Van Laer K, Oliveira M, Wahni K, Messens J The concerted action of a positive charge and hydrogen bonds dynamically regulates the pKa of the nucleophilic cysteine in the NrdH-redoxin family. *Protein Sci* 2014; **23**(2): 238–242.
- 55 Makmura L, et al. Development of a sensitive assay to detect reversibly oxidized protein cysteine sulfhydryl groups. *Antioxid Redox Signal* 2001; **3**(6): 1105–1118.
- 56 Doyle DA, et al. The structure of the potassium channel: molecular basis of K^+ conduction and selectivity. *Science* 1998; **280**(5360): 69–77.
- 57 Li D, Jin T, Gazgalis D, Cui M, Logothetis DE On the mechanism of GIRK2 channel gating by phosphatidylinositol bisphosphate, sodium, and the $\beta\gamma$ dimer. *J Biol Chem* 2019; **294**(49): 18934–18948.
- 58 Bernsteiner H, Zangerl-Plessl EM, Chen X, Stary-Weinzinger A Conduction through a narrow inward-rectifier K. *J Gen Physiol* 2019; **151**(10): 1231–1246.
- 59 Rosenhouse-Dantsker A, et al. A sodium-mediated structural switch that controls the sensitivity of Kir channels to PtdIns(4,5)P₂. *Nat Chem Biol* 2008; **4**(10): 624–631.
- 60 D'Avanzo N, Cheng WW, Doyle DA, Nichols CG Direct and specific activation of human inward rectifier K^+ channels by membrane phosphatidylinositol 4,5-bisphosphate. *J Biol Chem* 2010; **285**(48): 37129–37132.
- 61 Wang S, Lee SJ, Heyman S, Enkvetchakul D, Nichols CG Structural rearrangements underlying ligand-gating in Kir channels. *Nat Commun* 2012; **3**(1): 617.
- 62 Kostić D, et al. Xanthine oxidase: isolation, assays of activity, and inhibition. *J Chem* 2015; **2015**: 294858.
- 63 Fisher AB Redox signaling across cell membranes. *Antioxid Redox Signal* 2009; **11**(6): 1349–1356.
- 64 Takahashi MA, Asada K Superoxide anion permeability of phospholipid membranes and chloroplast thylakoids. *Arch Biochem Biophys* 1983; **226**(2): 558–566.
- 65 Lim JB, Langford TF, Huang BK, Deen WM, Sikes HD A reaction-diffusion model of cytosolic hydrogen peroxide. *Free Radic Biol Med* 2016; **90**: 85–90.
- 66 Yi BA, Lin YF, Jan YN, Jan LY Yeast screen for constitutively active mutant G protein-activated potassium channels. *Neuron* 2001; **29**(3): 657–667.
- 67 Franco R, Bortner CD, Cidlowski JA Potential roles of electrogenic ion transport and plasma membrane depolarization in apoptosis. *J Membr Biol* 2006; **209**: 43–58.
- 68 Brindeiro C, Fallet R, Lane P, Carmines P Potassium channel contributions to afferent arteriolar tone in normal and diabetic rat kidney. *Am J Physiol Renal Physiol* 2008; **295**(1): F171–178.
- 69 Brindeiro C, Lane P, Carmines P Tempol prevents altered K^+ channel regulation of afferent arteriolar tone in diabetic rat kidney. *Hypertension* 2012; **59**(3): 657–664.
- 70 Dobrev D, et al. The G protein-gated potassium current $I_{K,ACh}$ is constitutively active in patients with chronic atrial fibrillation. *Circulation* 2005; **112**(24): 3697–3706.
- 71 Voigt N, et al. Inhibition of $I_{K,ACh}$ current may contribute to clinical efficacy of class I and class III antiarrhythmic drugs in patients with atrial fibrillation. *Naunyn Schmiedebergs Arch Pharmacol* 2010; **381**: 251–259.
- 72 Mihm MJ, et al. Impaired myofibrillar energetics and oxidative injury during human atrial fibrillation. *Circulation* 2001; **104**(2): 174–180.